

A Lyapunov Based Approach to Enhance Wind Turbine Stability

A. Bennouk*, A. Nejmi, M. Ramzi

Mathematics and physics laboratory
Faculty of Sciences and Technics, Beni Mellal
Sultan Moulay Slimane University, Beni Mellal, Morocco
e-mail: bennouk.anasse@gmail.com

Abstract

This paper introduces a nonlinear control of a wind turbine based on a Double Feed Induction Generator. The Rotor Side converter is controlled by using field oriented control and Backstepping strategy to enhance the dynamic stability response. The Grid Side converter is controlled by a sliding mode. These methods aim to increase dynamic system stability for variable wind speed. Hence, The Doubly Fed Induction Generator (DFIG) is studied in order to illustrate its behavior in case of severe disturbance, and its dynamic response in grid connected mode for variable speed wind operation. The model is presented and simulated under Matlab/ Simulink.

Keywords: Double Fed Induction Generator, wind turbine, Rotor Side Converter, Lyapunov, Grid Side Converter

1. Introduction

Today, the number of wind turbines connected to the grid is steadily increasing. Variable speed wind turbines outperform constant speed turbines in aerodynamic efficiency while also reducing stress on the mechanical apparatus so as to make it more productive and cost-effective [1].

Double Fed induction generator (DFIGs) is becoming more used in modern wind power generation systems due to their variable speed operation, four quadrant active and reactive power regulation, low converter cost, and reduced power losses compared with Permanent Magnet Synchronous generators (PMSG).

Classic control of grid connected to DFIG is usually based on VOC (Voltage Oriented Control) or FOC (Flux Oriented Control), it decouples the d and q rotor currents in the synchronous frame. Control of instantaneous active and reactive power is then achieved by regulating the decoupled rotor currents, using proportional-integral (PI) parameters and accurate machine parameters. The weakness is shown when the machine's converters operate beyond their linear limits [1].

Field Oriented Control (FOC) is improved in this paper by the use of Backstepping strategy to control the Rotor Side inverter; this method has scored positive performances. This kind of control is generally associated with Lyapunov functions in order to increase system stability against variable wind fluctuations.

Moreover, Variable structure control or Sliding Mode Control (SMC) strategy is an effective and a high-frequency switching control for nonlinear systems showing uncertainties. It features simple implementation disturbance rejection, strong robustness and fast responses. This method will be used in the Grid Side inverter control so as to enhance Udc stability and then reach the grid parameters in term of frequency, Total Harmonics Distortion (THD) and voltage unbalance [2].

This paper is organized as follows: the second section is due to deal with a wind energy modeling under Matlab/Simulink. The third section illustrates the Field Oriented Control and Backstepping linearization control for the rotor side converter. The fourth section introduces a SMC destined to control of the Grid Side Converter performances. Finally, a simulation with its inherent results will be presented.

2. Wind Turbine Modeling

This section presents WECS based on a DFIG connected to the electric grid

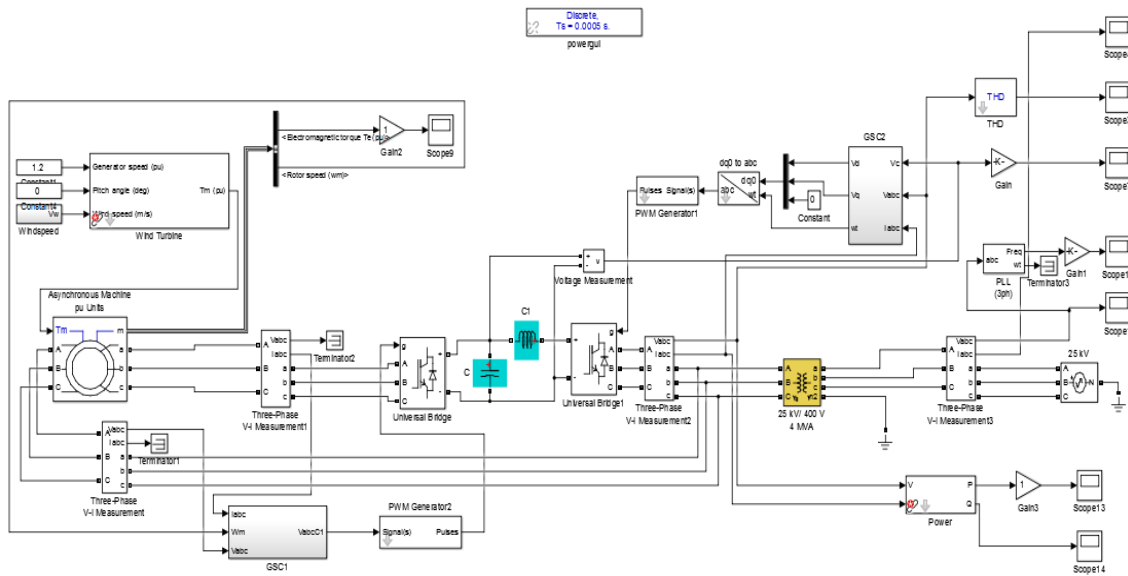


Figure 1. Wind turbine based on DFIG

Figure 1 shows the scheme of electrical energy's generation from the wind power on the basis of DFIG. As it is demonstrated, the stator is connected directly to the grid whereas the rotor is connected to the grid via a Back-to-back converter [2].

2.1. Wind Speed Model

Wind speed model contains four components [1]:

$$V_w(t) = V_b(t) + V_r(t) + V_n(t) + V_g(t) \tag{1}$$

where V_b is the base wind speed component (constant), V_r is the ramp wind component, V_n is the base noise wind component and V_g is the gust wind, V_g is set to zero during simulation, all of them in m/s. The model implementation of the wind speed in Matlab/Simulink is presented in Figure 2:

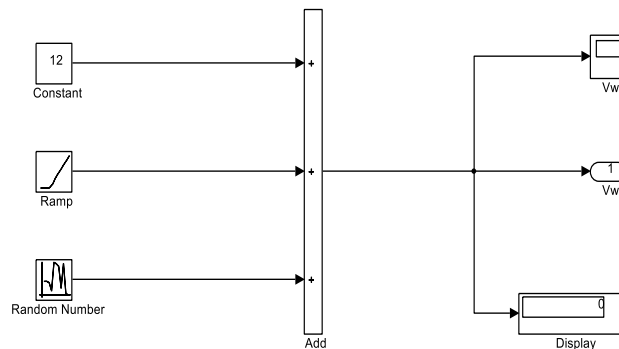


Figure 2. Wind speed model

The kinetic energy in this level is given by:

$$P_w = \frac{1}{2}mv^2 = \frac{1}{2}\rho Sv^3 \quad (2)$$

where m is the air mass, ρ is the air density, v is the wind speed and S is the covered surface of the turbine.

2.2. Wind Turbine Modeling

Wind turbine is applied to convert the wind energy into mechanical torque. The mechanical torque of the turbine can be calculated from mechanical power at the turbine extracted from wind power. Then, the power coefficient of the turbine (C_p) is used. The power coefficient is function of pitch angle (β) and tip speed (λ). The power coefficient maximum of (C_p) is known as the limit of Betz [2].

The power coefficient is given by:

$$C_p = C_1 \left(\frac{C_2}{\lambda_i} - C_3\beta - C_4 \right) e^{-\frac{C_5}{\lambda_i}} + C_6\lambda \quad (3)$$

where

$$\frac{1}{\lambda_i} = \frac{1}{\lambda + 0.08\beta} - \frac{0.035}{\beta_{3+1}} \quad \text{and} \quad \lambda = \frac{\omega_m \cdot R}{v}$$

C_1, C_2, C_3, C_4, C_5 and C_6 are constants given by the turbine constructor ($C_1 = 0.516, C_2 = 116, C_3 = 0.4, C_4 = 5.1, C_5 = 21$ and $C_6 = 0.0068$), R is the rotor radius and ω_m is the rotor speed generator. The power coefficient is a nonlinear function of the tip speed ratio λ and the blade pitch angle β (in degrees). If the swept area of the blade and the air density are constant, the value of C_p is a function of λ and it is maximum at the particular λ optimum. Hence, to fully utilize the wind energy, λ should be maintained at λ_{opt} , which is determined from the blade design, C_p is defined as [3]:

$$C_p = \frac{P_m}{P_w} \leq 1$$

and

$$P_m = \frac{1}{2}C_p\rho Sv^3 \quad (4)$$

where P_m is the mechanical output power of the turbine.

The Rotor Side converter is used to extract the MPPT (Maximum Power Point Tracking), in this purpose the DFIG angular speed reference is calculated permanently with an approach to follow the wind speed fluctuation, the wind turbine control generates the DFIG speed reference signal, performed by the RSC controller in DFIG control level. This reference signal is determined from the predefined characteristic $P-\omega$, based on filtered measured generator speed. Whereas the Grid Side Converter is used to control the DC link voltage and guarantees unity power factor in the rotor branch. The transmission of the reactive power from DFIG to the grid is thus only through the stator, a conventional vector with Lyapunov approach will be used in this command algorithm to enhance system stability.

3. Rotor Side Converter control

The standard vector control is used to control the RSC. In order to ensure stability when applying this control strategy mechanism, the stator flux magnitude must remain constant. To this purpose, Lyapunov's approach is used in order to enhance the system's stability [2].

The electrical energy conversion is described by the following equation according to a d-q frame :

$$V_{sd} = R_s i_{sd} + \frac{d\varphi_{sd}}{dt} - \omega_s \varphi_{sq} \quad (5)$$

$$V_{sq} = R_s i_{sq} + \frac{d\varphi_{sq}}{dt} + \omega_s \varphi_{sd}$$

$$V_{rd} = R_r i_{rd} + \frac{d\varphi_{rd}}{dt} - \omega_r \varphi_{rq}$$

$$V_{rq} = R_r i_{rq} + \frac{d\varphi_{rq}}{dt} + \omega_r \varphi_{rd}$$

and

$$\varphi_{sd} = L_s i_{sd} + L_m i_{rd} \quad (6)$$

$$\varphi_{sq} = L_s i_{sq} + L_m i_{rq}$$

$$\varphi_{rd} = L_r i_{rd} + L_m i_{sd}$$

$$\varphi_{rq} = L_r i_{rq} + L_m i_{sq}$$

Electromagnetic torque is expressed by:

$$T_e = \frac{P}{\Omega} = \frac{P.p}{\omega} = p(\varphi_{sd} i_{rq} - \varphi_{sq} i_{rd}) \quad (7)$$

V is the voltage, R_s and R_r are respectively the stator and rotor resistance. L_s, L_r and L_m are stator, rotor and mutual inductance between stator and rotor θ_s , and θ_r present angles of stator and rotor frames.

The aim of this approach is to catch the MPPT and to stabilize active power through regulating the electromagnetic torque depending basically on i_{rq} and i_{rd} , the stator flux is, thus, oriented to d axis in order to simplify the equations [5], [6]:

$$V_{sd} = 0 \text{ and } V_{sq} = \omega_s \varphi_{sq} \quad (8)$$

$$V_{rd} = R_r i_{rd} + \frac{d\varphi_{rd}}{dt} - \omega_r \varphi_{rq}$$

$$V_{rq} = R_r i_{rq} + \frac{d\varphi_{rq}}{dt} + \omega_r \varphi_{rd}$$

The new system inputs are respectively d-q rotor current and angular speed expressed by the following equations:

$$\frac{di_{rd}}{dt} - \frac{1}{L_r} v_{rd} - \frac{R_r}{L_r} i_{rd} + \omega_r i_{rq} \left(\frac{L_s L_r - M^2}{L_s L_r} \right) \quad (9)$$

$$\frac{d\varphi_{rq}}{dt} = V_{rq} - R_s i_{rd} - \omega_r \varphi_{rd}$$

$$\frac{di_{rq}}{dt} = -\frac{1}{L_r} v_{rq} + \left(\frac{M^2}{L_s L_r} - \omega_r \right) i_{rd} - \frac{M \omega_r}{L_r L_s \omega_s} V_{sq} - \frac{R_r}{L_r} i_{rq}$$

$$\frac{d\omega}{dt} = \frac{C_r}{J} - \frac{B}{J} \omega - \frac{K \varphi_{sd} i_{rq}}{J}$$

It is clear from the dynamic model above, the nonlinearity, because of the coupling between the d-q rotor currents and the speed, a variable change is initiated so as to introduce the Lyapunov function:

$$y_1 = \omega_c - \omega \quad (10)$$

$$y_2 = i_{rdref} - i_{rd}$$

$$y_3 = i_{rqref} - i_{rq}$$

ω is the angular speed, ω_c is the reference of ω , i_{rd} and i_{rq} are respectively the d and q axis rotor current, i_{rdref} and i_{rqref} are their references.

Lyapunov function is chosen as :

$$V_1 = \frac{1}{2}y_1^2 \quad (11)$$

$$\dot{V}_1 = y_1\dot{y}_1 = y_1(\dot{\omega}_c - Kp\varphi_{sd}i_{rq} + \frac{B}{J}\omega + \frac{Cr}{J}) \quad (12)$$

The derivative of the complete Lyapunov function is negative defined, if the quantities between parentheses in equation (12) are equal to zero. i_{qref} is given by:

$$i_{rqref} = \frac{1}{Kp\varphi_{sd}}(Cr + B.\omega + 2.J.K.y_1) \quad (13)$$

$$\dot{y}_2 = idref - i_{rd} - Ky_2 + Ky_2$$

and

$$\dot{y}_3 = iqref - i_{rq} - Ky_3 + Ky_3$$

V_2 and V_3 are defined respectively as :

$$V_2 = \frac{1}{2}y_2^2 \text{ and } V_3 = \frac{1}{2}y_3^2 \quad (14)$$

Lyapunov function is defined as:

$$V_4 = \frac{1}{2}(y_1^2 + y_2^2 + y_3^2) \quad (15)$$

$$\dot{V}_4 = -Ky_1^2 - Ky_2^2 - Ky_3^2 + y_2(idref - i_{rd} + Ky_2) + y_3(iqref - i_{rq} + Ky_3)$$

In order to fulfill Lyapunov's conditions, we integrate the following equations [2]:

$$A_1 = y_2(idref - i_{rd} + Ky_2) = 0 \quad (16)$$

and

$$A_2 = y_3(iqref - i_{rq} + Ky_3) = 0 \quad (17)$$

We conclude after calculating direct and quadrature voltage that :

$$V_{rd} = -KL_r y_2 - R_r i_{rd} + \omega_r \left(L_s L_r - \frac{M^2}{L_s L_r} \right) i_{rq} \quad (18)$$

$$V_{rq} = -KLry_3 + \left(\frac{M^2}{L_S L_r} - L_r \omega_r\right) i_{rd} + \frac{M\omega_r}{L_S \omega_S} V_{sq} + R_r i_{rq}$$

4. Grid Side Converter control

When the grid voltage changes suddenly, a control approach is adopted in the GSC to keep the DC voltage constant and to assure a zero rotor reactive power [7], [8], [9]. First, the system equations are defined as follows:

$$U_d = -L \frac{di_d}{dt} - R i_d + \omega L i_q + v_d \quad (19)$$

$$U_q = -L \frac{di_q}{dt} - R i_q - \omega L i_d + v_q$$

$$C \frac{d}{dt} v_{dc} = i_{dc} = i_L - i_d$$

U_d, U_q :d-q components of converter voltage

v_d, v_q : d-q grid voltage components

i_d, i_q :d-q current components

We suppose that the grid voltage is aligned to the d-axis. We may define the state system as [10]:

$$\begin{bmatrix} i_d \\ i_q \\ v_{dc} \end{bmatrix} = \begin{bmatrix} -R/L & \omega \\ \omega & -R/L \\ -1/C & 0 \end{bmatrix} \begin{bmatrix} i_d \\ i_q \end{bmatrix} + \begin{bmatrix} -\frac{U_d}{L} + \frac{v_d}{L} \\ -1/LUq \\ i_L \end{bmatrix} \quad (20)$$

$$y_1 = i_d \quad (21)$$

$$y_2 = v_{dc} + i_q - i_L$$

$$S_1 = y_{1ref} - y_1 \quad (22)$$

$$S_2 = y_{2ref} - y_2$$

In order to keep the system stability, the sliding system should be:

$$S_2 \cdot \dot{S}_1 \leq 0 \text{ and } S_2 \cdot \dot{S}_2 \leq 0$$

Then we deduce the U_d and U_q :

$$U_d = K \text{sign}(S_1) - R i_q + L \omega i_d + v_d \quad (23)$$

$$U_q = K \text{sign}(S_2) + i_d L \left(\omega - \frac{1}{C}\right) - R i_q + (i_L - i_d)$$

5. Simulation and results

The test wind profile with full field turbulence is generated through the use of Wind turbine block as presented in Figure 1. This block shows the hub height wind speed profile. In general, wind speed consists of two components, mean wind speed and turbulence component. The simulation is realized in order to illustrate Grid parameters stability, Grid voltage unbalance, THD and Frequency.

The wind turbine and DFIG parameters are illustrated in Table 1 [11]:

Table 1. DFIG parameters

Parameter	Symbol	Value
Active Power	P	2MW
Stator resistance	R_s	0.001518 Ω
Stator inductance	L_s	0.059906 H
Rotor inductance	L_r	0.082060 H
Rotor resistance	R_r	0.002087 Ω
Mutual inductance	L_m	2.4 H
Pole pairs	N	2
Inertia	J	17.23Kg.m ²
Gear box	n_g	5.065

Simulation and results are presented first with a constant wind profile, then during a variable wind speed to illustrate the used approach robustness based on Lyapunov theory:

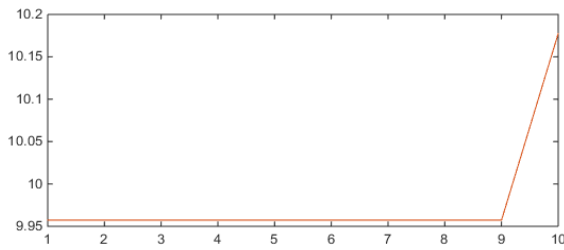


Figure 3. Wind speed

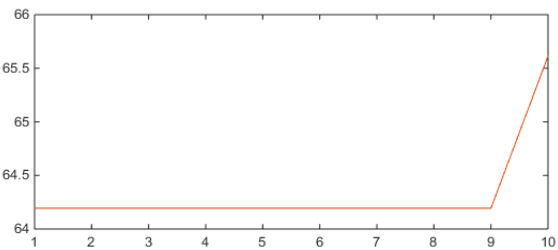


Figure 4. Rotor angular speed

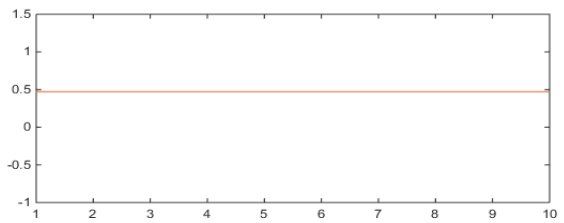


Figure 5. Power Coefficient (Cp)

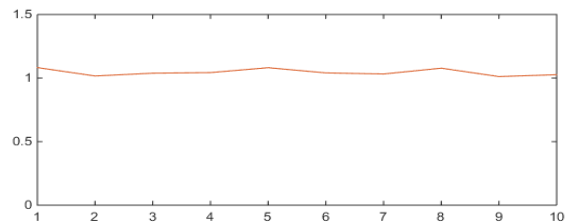


Figure 6. Vdc

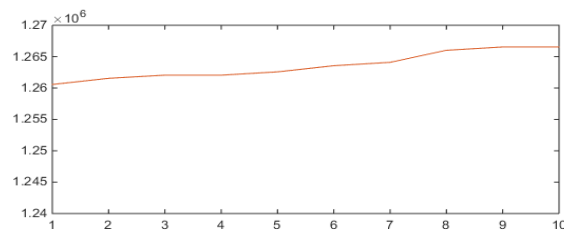


Figure 7. Active Power

It's obvious that for a constant wind speed, the wind power captured and delivered to the grid had the same shape as the wind, active power is kept constant and equal to 1.26MW for a wind speed of 9.9m/s, the MPPT approach is well achieved and the power coefficient is maintained at 0.47. The DFIG speed is the image of the wind speed, it is following properly its reference. Lyapunov approach used to control GSC shows also good performances and the Udc voltage was equal to its reference .

We present here simulations result following variable wind speed :

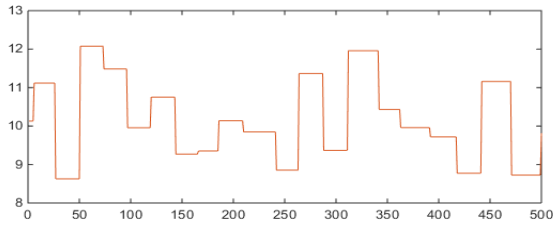


Figure 8. Variable wind speed

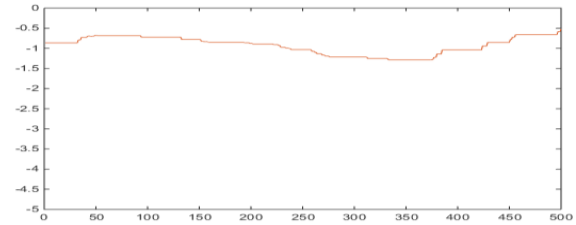


Figure 9. Electromagnetic torque

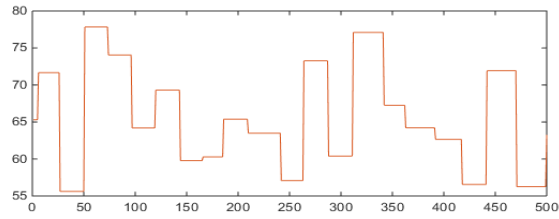


Figure 10. Rotor angular speed

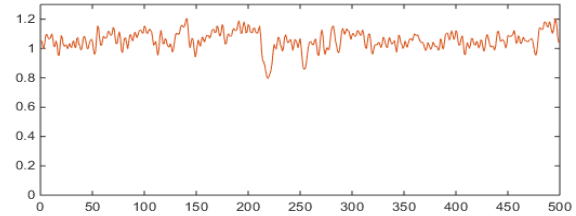


Figure 11. Vdc voltage

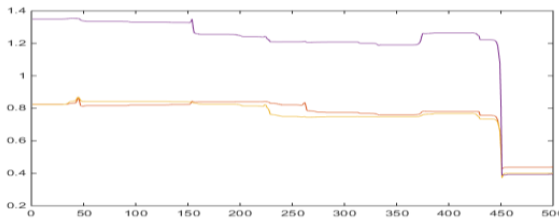


Figure 12. Total Harmonics Distorsion (THD)

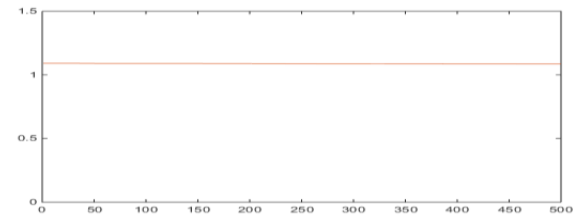


Figure 13. Frequency

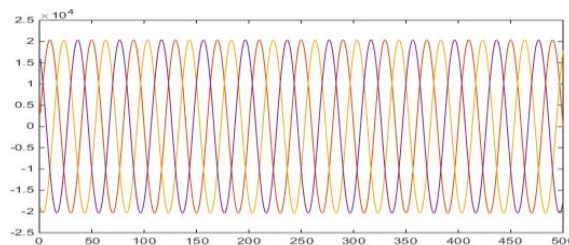


Figure 14. Grid voltage

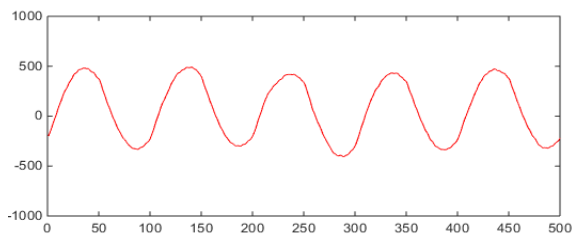


Figure 15. Grid Current

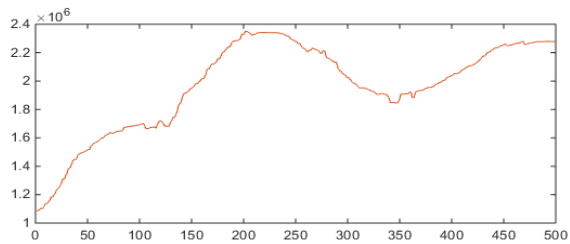


Figure 16. Active power

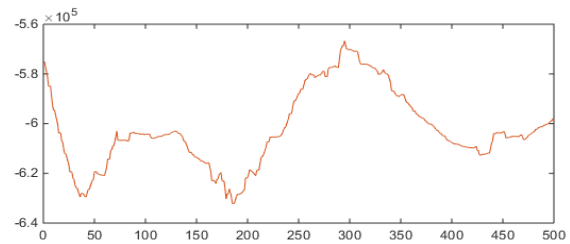


Figure 17. Reactive power

The dynamic responses of the DFIG generation system under an intermittent wind action are shown in Figure 8. It is clear that when a mean wind speed changes, the electromagnetic torque varies. We may deduce then that when the wind speed increases 11m/s, the electromagnetic field is set at 1pu. Consequently, the delivered power is more or equal to 2MW. Conversely, when the wind speed is inferior, the electromagnetic and active power generated decreases proportionally. The DFIG speed is the image of the wind speed, it is following properly its reference

The DC link voltage also varies according to the wind speed fluctuations, but the variation is not obvious as shown in Figure 11. The DC voltage is generally kept at its reference.

The Total Harmonic Distortion presented in Figure 12 had demonstrated good performances and did not exceed 5%, the assigned threshold of national grid code. The frequency, as shown in Figure 13, did not also exceed the threshold of 1.2 pu. The grid side voltage had shown also good performances apart from some a slight distortion caused by dynamic response and wind speed fluctuations. The balance voltage remained inferior to 1%, which is the fixed threshold of National Grid Code [2].

The active power variations illustrated in Figure.16 depend and follow the wind speed variation which has demonstrated also good performances. The active power reaches its highest values when the wind speed exceeds 11m/s.

The reactive power had shown a good performance as presented in Figure.17 except in 200s, when we observe that the reactive power exceeds 600 Kvar following a quick fluctuation of Udc link voltage.

6. Conclusion

With the growing level of penetration scored by wind-origin power production into the general power system, many national codes have been applied so as to ensure stability to the electric grid. Many simulations and complete models are needed to be established prior to any connection between wind farm and electric grid [2].

A nonlinear control of variable speed WT is, thus, proposed. The main aim here is to maximize the energy capture from the wind while reducing Grid parameters deviations.

Also, and with the aim of illustrating from one side the system stability and to what extend it matches the national grid code, we have identified and presented the THD, frequency and voltage unbalance in the Point of Common Coupling (PCC), as these parameters had shown when they were under their limit during the simulation time.

Stability had been improved by using FOC and Lyapunov conditions in the Generator Side Converter. In the Grid Side Converter, SMC control was applied. The different PID controllers had been turned so as to obtain good performances. The use of SMC associated to Lyapunov had also demonstrated good performances in terms of Grid parameters stability.

References

- [1] Hu J, Nian H, Hu B, He Y, Zhu ZQ. Direct Active and Reactive Power Regulation of DFIG Using Sliding –Mode Control. *IEEE*. 2010; 25(4): 1028-1039.
- [2] Bennouk A, Nejmi A, Benamou A, Ramzi M. Backstepping and MIMO approaches to control a wind turbine based on DFIG. *International Journal of Emerging Technology and Advanced Engineering*. 2016; 6(3): 12-17.
- [3] Mullane A, Lightbody G, Yacamini R. Adaptive Control of Variable Speed Wind Turbines. *Rev. Energ.: Ren. Power Engineering*. 2001; 101-110.
- [4] Bossouf B, Karim M, Lagrioui A and Taoussi M. Backstepping Control of DFIG Generators for Wide-Range Variable-speed Wind Turbines. *Int. J. Automation and Control*. 2014; 8(2): 122-140.
- [5] Song Y.D, Dhinakaran B, Bao X.Y. Variable speed control of wind turbines using nonlinear and adaptive algorithms. *Journal of Wind Engineering and Industrial Aerodynamics*. 2000; 293-308.
- [6] Beltran B, Ahmed-Ali T, Benbouzid M. Sliding Mode Power Control of Variable-Speed Wind Energy Conversion Systems. *IEEE Transaction Energy Conversion*. 2008; 23 (8): 551-558.
- [7] Khemiri N, Kheder A, Faouzi M. An Adaptive Nonlinear Backstepping Control of DFIG Driven by Wind Turbine. *WSEAS Transactions on Environment and Development*. 2012; 8(2): 60-71.
- [8] Beltran B, Ali T, Benbouzid M. Sliding Mode Power Control of Variable-Speed Wind Energy Conversion Systems. *IEEE*. 23(2): 551-558.
- [9] Rajendran S, Jena D. Backstepping Sliding Mode Control of a Variable Speed Wind Turbine For Power Optimization. *Journal of Modern Power Systems and Clean Energy*. 2015; 3(3):402–410
- [10] Sung-Hun L, Jun Joo Y, Juhoon Back, Jin-Heon S, Ick C. Sliding Mode Controller for Torque and Pitch Control of PMSG Wind Power Systems. *Journal of Power Electronics*. 2011; 11(3): 342-349.
- [11] Li S, Haskew T.A, Williams K.A, Swatloski R.P. Control of DFIG Wind Turbine With Direct-Current Vector Control Configuration. *IEEE*. 2012; 3(1): 1-11.